Fundamental Transmitting Properties of Carbon Nanotube Antennas

G. W. Hanson, *Senior Member, IEEE*

Abstract—**Fundamental properties of dipole transmitting antennas formed by carbon nanotubes are investigated. Since carbon nanotubes can be grown to centimeter lengths, and since they can be metallic, the properties of carbon nanotubes as antenna elements are of fundamental interest. In this paper, dipole carbon nanotube antennas are investigated via a classical Hallén's-type integral equation, based on a quantum mechanical conductivity. The input impedance, current profile, and efficiency are presented, and the radiation pattern is discussed, as are possible applications.**

Index Terms—**Carbon nanotube, dipole antennas, electromagnetic theory, nanotechnology.**

I. INTRODUCTION

CARBON nanotubes (CNs) were discovered in 1991 [1] and have since lead to an enormous amount of research into their fundamental properties. Roughly speaking, a single-wall carbon nanotube (SWNT) is a rolled-up sheet of graphene (i.e., a monoatomic layer of graphite) having a radius of a few nanometers and lengths (so far) up to centimeters [2]. Thus, their length to radius ratio can be on the order of 10^7 or more. Multiwalled carbon nanotubes (MWNTs), carbon nanotube ropes, and other related structures also exist, although attention here will be focused on SWNTs.

At an atomic level, graphene has the honeycomb structure shown in Fig. 1, where the small circles denote the location of carbon atoms and the lines depict carbon–carbon bonds [3]. Lattice basis vectors are $\mathbf{a}_1$ and $\mathbf{a}_2$, as shown, and the relative position vector is $\mathbf{R} = m\mathbf{a}_1 + n\mathbf{a}_2$, where m, n are integers. A carbon nanotube can be formed by wrapping the graphene sheet into a cylinder (of course, carbon nanotubes form naturally in, for example, the arc discharge of carbon electrodes and are not made by literally rolling graphene sheets into cylinders).

Obviously, the cylinder can be formed by wrapping the sheet along any preferred axis. If the cylinder axis is the ξ axis in Fig. 1, the resulting tube is called a zigzag CN. If the cylinder axis is the η axis in Fig. 1, the resulting tube is called an armchair CN. If the cylinder axis is neither the ξ nor the η axis as shown, the resulting nanotube is called a chiral CN. Thus, carbon nanotubes can be characterized by the dual index (m, n), where $(m, 0)$ for zigzag CNs, (m, m) for armchair CNs, and (m, n),
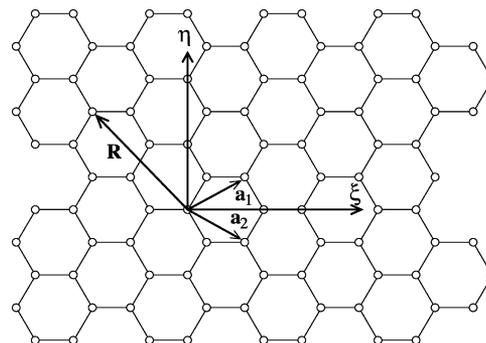
Fig. 1. Graphene sheet showing coordinate system, lattice basis vectors, and position vector. Circles denote the positions of carbon atoms.

$0 < n \neq m$, for chiral nanotubes. The resulting cross-sectional radius of a carbon nanotube is given by [3]

$$a = \frac{\sqrt{3}}{2\pi} b \sqrt{m^2 + mn + n^2} \tag{1}$$

where $b = 0.142$ nm is the interatomic distance in graphene.

Electrically, carbon nanotubes have fascinating properties. For example, they can be either metallic or semiconducting, depending on their geometry (i.e., on m, n) [3], [4]. Armchair CNs are always metallic (they exhibit no energy bandgap), as are zigzag CNs with $m = 3q$, where q is an integer. Furthermore, carbon nanotubes can exhibit dc ballistic transport [3] over at least micrometer lengths. When ballistic transport occurs, the resistance of the tube is independent of length and is, theoretically, approximately 6.45 kΩ. This resistance value results from having two propagation bands (called the π-bands) forming parallel propagation channels, where each channel has resistance equal to the resistance quantum [5], $R_0 \simeq 12.9$ kΩ. Carbon nanotubes have been made into transistors [6], [7], gas sensors [8], nanotweezers [9], and field emission devices [10], among other uses.

Whereas the dc and optical properties of carbon nanotubes have been studied both experimentally and theoretically, their radio-frequency properties have not been considered as thoroughly [6], [11]. Since carbon nanotubes can be grown having lengths on the order of a centimeter, and can be metallic, a natural topic is to consider carbon nanotubes for centimeter and millimeter-wave antenna applications, as originally proposed in [12].

In [12], carbon nanotube dipole antennas were considered based on a transmission-line model. In this method, two parallel conductors form a transmission line, and the transmission-line parameters' inductance L, capacitance C, and resistance R are

determined for the line, based on the line geometry and materials. Then, the usual transmission-line quantities, such as propagation constant, phase velocity, and characteristic impedance, are determined. The transmission-line current due to an open-circuited end is obtained and used to model the flared-out transmission line, which forms a dipole antenna. The radiated field can then be obtained, and other antenna parameters determined from the approximate current distribution, which is a standing wave in the lossless case. Transmission-line modeling of carbon nanotubes is further considered in [13] and [14] and references therein.

As noted in [12], several effects make the carbon nanotube transmission line act differently from an ordinary metallic transmission line. Without going into detail, for a carbon nanotube transmission line there exists a kinetic inductance L_K that dominates over the usual magnetic inductance [12]. Also, both the usual electrostatic capacitance and a quantum capacitance must be taken into account. One result is that the wave velocity on a carbon nanotube transmission line is on the order of the Fermi velocity v_F rather than the speed of light c (here we assume that the transmission line exists in free space). For a CN, $v_F \simeq 9.71 \times 10^5$ m/s; as explained later, here we find that the propagation velocity on a carbon nanotube dipole is $v_p \simeq 6.2 v_F \simeq 0.02c$. Thus, wavelengths are much shorter on a carbon nanotube, compared to on a typical macroscopic metallic tube.

In this paper, fundamental properties of finite-length dipole antennas formed by carbon nanotubes are investigated using a Hallén's-type integral equation. The input impedance, current profile, and efficiency are presented and compared to ordinary metallic antennas of the same size and shape. Possible applications of carbon nanotube antennas are discussed. The carbon nanotube is accounted for using a semiclassical conductivity derived explicitly for infinite carbon nanotubes [15], [16]. At the frequencies of interest in this paper, this semiclassical conductivity is equivalent to the more rigorous (and complicated) quantum mechanical conductivity also derived in [15] and [16], which accounts for interband transitions ignored in the semiclassical analysis. The integral equation method utilized here can be considered as being, overall, a semiclassical technique, since the classical Maxwell's equations are used. This formulation should be accurate through terahertz frequencies, although at higher frequencies (and, therefore, involving higher energy photons), interband transitions should be taken into account using the full quantum conductivity. This paper is a considerably expanded version of [17], all units are in the SI system, and the time variation (suppressed) is $e^{j\omega t}$.

II. FORMULATION

The integral equation that is ultimately solved [(31)] is similar to the well-known integral equation for a metal-tube antenna. However, it is instructive to derive the integral equation in order to appreciate the difference between a carbon nanotube and a metallic tube. We will consider a two-dimensional (infinitely thin) tube, in the form of a circular cross-sectional cylinder of radius a and oriented along the z axis, as shown in Fig. 2.
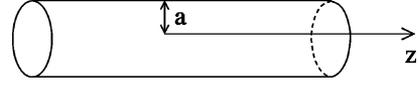
Fig. 2. Carbon nanotube and metallic tube geometry.

Following [15] and [16], the conductivity is derived starting with Boltzmann's equation [18], [19], specialized to the case of a z-directed electric field E_z and resulting current flow solely in the z direction under the relaxation-time approximation

$$\frac{\partial f}{\partial t} + eE_z\frac{\partial f}{\partial p_z} + v_z\frac{\partial f}{\partial z} = \nu\left[f_0(\mathbf{p}) - f(\mathbf{p}, z, t)\right] \quad (2)$$

where f is the electron's distribution function, v_z is the electron's velocity, e is the electron's charge, ν is the relaxation frequency ($\nu = \tau^{-1}$, where τ is the relaxation time), and $\mathbf{p}$ is the two-dimensional electron momentum. In (2), f_0 is the Fermi–Dirac distribution

$$f_0(\mathbf{p}) = \left(1 + e^{\frac{E(\mathbf{p})-E_F}{k_B T}}\right)^{-1} \quad (3)$$

where E_F is the Fermi energy, $E(\mathbf{p})$ is the electron's energy, k_B is Boltzmann's constant, and T is temperature. As discussed in [15] and [16], this semiclassical (not fully quantum-mechanical) model describes only intraband motion of electrons, which is, however, sufficient at the frequencies of interest here. Writing $E_z = \text{Re}(E_z^0 e^{j\omega t})$ and $f = f_0 + \text{Re}(\delta f e^{j\omega t})$, where δf is a small quantity, and inserting into (2) leads to

$$\delta f = j\frac{\partial f_0}{\partial p_z}\frac{eE_z^0}{\omega - j\nu}. \quad (4)$$

The axial current density (in two dimensions) is [18]

$$J_z = \frac{2e}{(2\pi\hbar)^2}\int\int v_z f d^2\mathbf{p} \quad (5)$$

where $\hbar$ is the reduced Planck's constant. Writing $J_z = \text{Re}(J_z^0 e^{j\omega t})$ and $J_z^0 = \sigma_{zz}(\omega)E_z^0$, we have [15], [16]

$$\sigma_{zz}(\omega) = j\frac{2e^2}{(2\pi\hbar)^2}\int\int\frac{\partial f_0}{\partial p_z}\frac{v_z}{\omega - j\nu}d^2\mathbf{p}. \quad (6)$$

Although the derivation in [15] and [16] is aimed at carbon nanotubes, it is fairly general [18], applying to any two-dimensional (infinitely thin) material that can be modeled using the relaxation-time approximation of Boltzmann's equation. The specific material type comes into play by specifying the energy-momentum relationship $E(\mathbf{p})$, and the Fermi energy E_F, in (6).

In particular, for the carbon nanotube, $E_F = 0$, and $E(\mathbf{p})$ is specified by

$$E(p_z, s) = \pm\gamma_0\sqrt{1 + 4\cos(\xi_z^a)\cos(\xi_s) + 4\cos^2(\xi_s)} \quad (7)$$

for zigzag CNs and

$$E(p_z, s) = \pm\gamma_0\sqrt{1 + 4\cos(\xi_z^b)\cos(\xi_s) + 4\cos^2(\xi_z^b)} \quad (8)$$

for armchair CNs, where γ_0 is a constant ($\gamma_0 \backsim 2.7 - 3eV$), $\xi_z^a = 3bp_z/(2\hbar)$, $\xi_z^b = \sqrt{3}bp_z/(2\hbar)$, and $\xi_s = \pi s/m$, and

where $s = 1, 2, \ldots, m$ accounts for the quantized momentum in the circumferential direction. For small radius carbon nanotubes ($m < 50$), (6) can be approximated by [15], [16]

$$\sigma_{cn}(\omega) = \sigma_{zz}(\omega) \simeq -j\frac{2e^2 v_F}{\pi^2 \hbar a(\omega - j\nu)} \qquad (9)$$

where v_F is the Fermi velocity for a CN. Although Boltzmann's equation is collision-driven, and therefore most applicable at frequencies $\omega < \nu$, the result (9) agrees with a quantum mechanical expression through terahertz frequencies [15], [16]. Note that the units of σ_{cn} are siemens (S), rather than S/m, since the carbon nanotube is modeled as an infinitely thin tube supporting a surface current density.

As a comparison to (9), the conductivity of a two-dimensional (infinitely thin) metal cylinder will be derived, starting from (6). In this case, quantization in the circumferential direction can be ignored as a first approximation, since we assume that the circumference of the metal cylinder is much greater than the electron's de Broglie wavelength λ_e. Since λ_e is on the order of 0.5 nm for copper in both two and three dimensions, this should be a reasonable approximation. The interpretation of the resulting conductivity is described later.

The well-known Fermi-gas model of electrons in metals leads to [18]

$$E(\mathbf{p}) = \frac{\hbar^2}{2m}\left(p_z^2 + p_y^2\right) \qquad (10)$$

which is derived by applying Schrödinger's equation to noninteracting electrons in an infinite (in this case, two-dimensional) region of space. Using (10), changing to polar coordinates and making the standard approximation

$$\left(-\frac{\partial f_0(E)}{\partial E}\right) = \delta(E_F - E) \qquad (11)$$

yields the result

$$\sigma_{2d}(\omega) = \sigma_{zz}(\omega) = -j\frac{e^2 E_F}{\pi \hbar^2 (\omega - j\nu)} \qquad (12)$$

where σ_{2d} denotes the two-dimensional conductivity for a Fermi-gas metal such as copper. Using the Fermi energy in two dimensions [20], [21], $E_F = N_e^{2d} \pi \hbar^2 / m_e$, we have

$$\sigma_{2d}(\omega) = -j\frac{e^2 N_e^{2d}}{m_e(\omega - j\nu)} \qquad (13)$$

where N_e^{2d} is the number of elections per m^2 and m_e is the mass of an electron. It is interesting to note that, although the details of the derivation would change slightly, for a three-dimensional conductor the three-dimensional version of (6) leads to an analogous result

$$\sigma_{3d}(\omega) = -j\frac{e^2 N_e^{3d}}{m_e(\omega - j\nu)} \qquad (14)$$

although in that case N_e^{3d} is the three-dimensional electron density $(N_e^{2d} = (N_e^{3d})^{2/3})$ such that the units of σ_{3d} are S/m. In either case the well-known semiclassical result for static conductivity (which is also identical to the classical result) [18], $\sigma(0) = e^2 N_e \tau/m$, is recovered for $\omega = 0$, and the usual frequency dependence [19], $\sigma(\omega) = \sigma(0)[(1 - j\omega\tau)/(1 + (\omega\tau)^2)]$ is reproduced by (13) and (14). For copper, $N_e^{3d} \simeq 8.46 \times 10^{28}$ electrons/m^3 [19].

The integral equation for current density can be obtained from Ohm's law

$$J_z(z, \omega) = \sigma(\omega) E_z(z, \omega) \qquad (15)$$

for all z along the tube, where σ denotes either σ_{cn} for the carbon nanotube or σ_{2d} for a metal tube and J_z is a surface current density (A/m). Actually, the conductivity developed for the nanotube (9) applies to an infinitelylong tube. End effects will alter the energy band structure near the tube ends, changing the conductivity. However, for a long nanotube antenna this effect can be expected to be small, and is ignored here. However, caution should be exercised when considering carbon nanotubes in the proximity of nearby objects, since the energy band structure may be strongly affected, although this is a matter requiring further research.

The remainder of the formulation follows standard antenna analysis. Starting with [22]

$$\mathbf{E}(\mathbf{r}) = \frac{1}{j\omega\varepsilon}(k^2 + \nabla\nabla\cdot)\int_V g(\mathbf{r}, \mathbf{r}')\mathbf{J}(\mathbf{r}')dV' \qquad (16)$$

where

$$g(\mathbf{r}, \mathbf{r}') = \frac{e^{-jkR}}{4\pi R} \qquad (17)$$

$R = |\mathbf{r} - \mathbf{r}'|$, and writing $\mathbf{J}(\mathbf{r}) = \hat{\mathbf{z}}J_z(z)\delta(\rho - a)$, we obtain

$$E_z = \frac{1}{j4\pi\omega\varepsilon}\left(k^2 + \frac{\partial^2}{\partial z^2}\right)\int_{-L}^{L} K(z - z')I(z')dz' \qquad (18)$$

where L is the half-length of the antenna. In (18)

$$K(z - z') = \frac{e^{-jk\sqrt{(z-z')^2+a^2}}}{\sqrt{(z-z')^2 + a^2}} \qquad (19)$$

is the standard thin-wire kernel, which will be appropriate here since the radius a will be on the order of a nanometer (the thin-wire kernel and Hallén's integral equation are discussed in [23]) and where

$$I(z) = J_z(z)2\pi a. \qquad (20)$$

Ohm's law (15) is then

$$\frac{I(z)}{2\pi a} = \sigma\left(E_z^s(z) + E_z^i(z)\right) \qquad (21)$$

where E_z^i is an incident field and E_z^s is the scattered field. Writing the scattered field as (18), we have the Pocklington integral equation

$$\left(k^2+\frac{\partial^2}{\partial z^2}\right)\int_{-L}^{L} K(z-z')I(z')dz' = j4\pi\omega\varepsilon\left(z_iI(z)-E_z^i(z)\right)$$

(22)

where

$$z_i = \frac{1}{2\pi a\sigma}$$

(23)

is the antenna's impedance per unit length. The above integral equation is identical in form to the Pocklington equation for an imperfectly conducting finite-thickness tubular wire antenna [24]. In that case, however, rather than (23) for the infinitely thin tube, if the metal tube's wall thickness is d

$$z_i = \frac{1}{2\pi a(\sigma_{3d}d)}$$

(24)

if d is thin compared to the skin depth, $\delta_s = (2/\omega\mu\sigma_{3d})^{1/2}$ [24], and

$$z_i = \frac{1+j}{2\pi a(\sigma_{3d}\delta_s)}$$

(25)

if d is much greater than the skin depth.

Therefore, from the preceding derivation we can see that the two-dimensional conductivity (σ_{2d} for an infinitely thin metal tube or σ_{cn} for the carbon nanotube) plays the same role as the product of bulk conductivity σ_{3d} and wall thickness (i.e., $\sigma_{3d}d$) or bulk conductivity σ_{3d} and skin depth (i.e., $\sigma_{3d}\delta_s$) for a finite-thickness metal tube. This is consistent with the idea of a sheet conductivity $\sigma_{\text{sheet}} = \sigma_{\text{bulk}}t$, where t is a thickness parameter. Note that (22) also holds for a solid cylindrical conductor if one uses the impedance [24]

$$z_i = \frac{\gamma J_0(\gamma a)}{2\pi a\sigma_{3d}J_1(\gamma a)}$$

(26)

where

$$\gamma = (1-j)\sqrt{\frac{\omega\mu\sigma_{3d}}{2}}$$

(27)

and where J_0 and J_1 are the usual first-kind Bessel functions.

At this point it is instructive to consider in more detail the conductivities (9), (13), and (14). In particular, (9) is the surface conductivity (S) of the carbon nanotube. Since the wall of an actual single-walled CN is a monoatomic sheet of carbon, and since high-quality carbon nanotubes can be grown (i.e., without significant defects or impurities), the resulting infinitely thin surface conductivity model should be valid.

For a carbon nanotube, the relaxation frequency is taken as $\nu = (3\times10^{-12})^{-1}$ [16], and here we use $v_F \simeq 9.71\times10^5$ m/s. The carbon nanotube conductivity σ_{cn} for armchair tubes with various $n = m$ values is shown in Fig. 3(a), where, for example, for $m = 5$, $a = 0.339$ nm, and for $m = 40$, $a = 2.712$ nm.
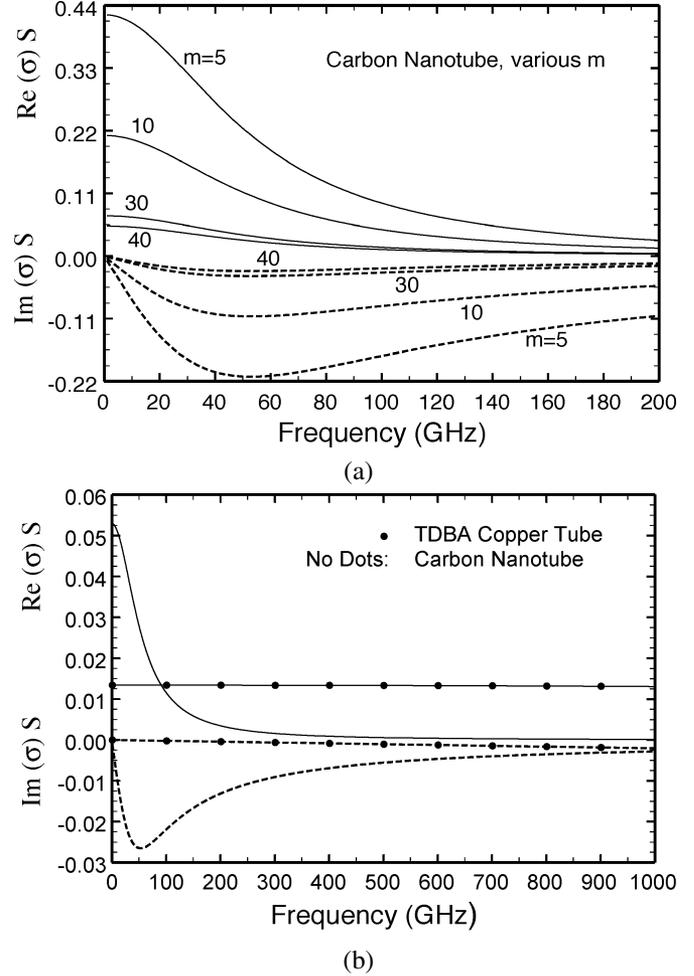
Fig. 3. (a) Conductivity (9) as a function of frequency for carbon nanotubes, for various m values (i.e., various radius values). Solid lines are Re(σ); dashed lines are Im(σ). (b) Conductivity σ_{cn} (9) as a function of frequency for carbon nanotubes, $m = 40$ ($a = 2.712$ nm), and σ_{2d}, (13), for an infinitely thin two-dimensional bulk approximation copper tube having the same radius. Solid lines are Re(σ); dashed lines are Im(σ).

In order to provide a comparison to the CN results, it would be useful to make a comparison to a metal dipole of the same size and shape. However, the interpretation of the copper tube model at the nanoscale needs some explanation. In contradistinction to the case of a macroscopic metal dipole, the value of conductivity plays an important role for nanometer radius antennas. Keeping in mind that $\sigma_{3d} \sim O(10^7)$, it is clear from (24)–(26) that if a becomes very small, $|z_i|$ will be relatively large, significantly alternating the antenna's properties from the perfectly conducting ($z_i = 0$) case.

As a concrete example, consider a solid copper dipole antenna that has total length 0.47λ, so that it is approximately at resonance, and assume $F = 160$ GHz. When $a = 0.002\lambda$ (i.e., $a = 3.75$ μm), there is not much difference in the input impedance assuming a perfect conductor Z_{in}^{pc} and the input impedance assuming bulk copper Z_{in}^σ, as shown in Table I [results were obtained from (31) assuming the solid conductor impedance (26)]. This is why, generally, antennas can be well approximated as perfect conductors at radius values of typical

INPUT IMPEDANCE AND EFFICIENCY FOR A SOLID CYLINDRICAL METAL WIRE APPROXIMATELY NEAR RESONANCE (TOTAL LENGTH IS 0.47λ), FOR MICROMETER AND NANOMETER RADIUS VALUES. Z_{in}^{pc} AND Z_{in}^{σ} ARE THE PERFECTLY-CONDUCTING AND BULK COPPER APPROXIMATIONS, RESPECTIVELY

Radius	Input Impedance (ohms)	$e_r = P_r/P_{in}$
3.75 μm	$Z_{in}^{pc} = 69.84 - j7.36$	1.00
	$Z_{in}^{\sigma} = 72.24 - j5.76$	0.97
20 nm	$Z_{in}^{pc} = 62.78 - j76.96$	1.00
	$Z_{in}^{\sigma} = 1,960.13 - j1,917.14$	5.53×10^{-3}
2 nm	$Z_{in}^{pc} = 62.08 - j106.85$	1.00
	$Z_{in}^{\sigma} = 19,788.96 - j19,539.85$	4.82×10^{-6}

interest (usually larger than a micrometer). However, for very small radius values, $|z_i|$ becomes very large, such that Z_{in}^{σ} and Z_{in}^{pc} have very different values, as can be seen from the table for the $a = 20$ nm and $a = 2$ nm cases (the use of the bulk copper approximation in computing Z_{in}^{σ} will be discussed below).

Also shown in the table is the efficiency $e_r = P_r/P_{in}$, where P_r is the power radiated and P_{in} is the power input

$$P_{in} = \frac{1}{2}\text{Re}(Z_{in})I_0^2 \tag{28}$$

with I_0 being the current at the feed point. It is clear, then, that, although good agreement is generally found between measurements of a real metal dipole and simulation results assuming a perfect conductor, this will only be true for radius values on the order of a micrometer or larger. In fact, in order for the perfect conductor and imperfect conductor models to give reasonable agreement at nanometer radius values, the conductivity of the material would need to be several orders of magnitude larger the bulk copper value. Therefore, for nanometer radius antennas, one must account for the finite conductivity of the material rather than assuming a perfect conductor model.

However, at this time, the value of conductivity for nanometer radius wires is unknown. For example, recent measurements on rectangular cross-section copper traces indicate that when lateral dimensions fall below 100 nm, surface and grain boundary scattering cause a significant increase in resistivity. In particular, for 50×50 nm copper traces, the resistivity was approximately twice as large as the bulk value for copper [25]. Furthermore, resistivity was shown to increase sharply as dimensions were reduced, although no values were presented under 40 nm. There will also be a strong influence of impurities and material imperfections in fabricating extremely small dimension copper traces. Therefore, at this time, it is impossible to have a realistic value of conductivity to use for the copper dipole at nanometer radius values, and it is clear that the usual perfect conductor approximation is not meaningful. To provide a contrast to the CN results, and to avoid somewhat arbitrarily choosing a value of conductivity, the bulk conductivity of copper will be used. That is, (13) will be used, where $\nu \simeq (2.47 \times 10^{-14})^{-1}$, which is the bulk copper value [19]. However, it should be recognized that the resulting conductivity may be far too large. This material, described by σ_{2d}, will be called the two-dimensional bulk approximation (TDBA) copper.

Fig. 3(b) shows a plot of conductivity as a function of frequency for armchair tubes with $n = m = 40$ [leading to $a =$

2.712 nm from (1)] and for an infinitely thin TDBA copper tube of the same radius. In particular, at $F = 10$ GHz, for $m = 40$ we have $\sigma_{cn} = 0.0512 - j0.009\,64$ S. For comparison, the TDBA copper value is, from (13), $\sigma_{2d} = 0.0134 - j0.000\,021$ S. Therefore, at this frequency, the carbon nanotube conductivity σ_{cn} (at least the real part) is on the same order of magnitude as the TDBA copper sheet conductivity σ_{2d}, although σ_{cn} is quite dispersive compared to σ_{2d}. From (14), the bulk conductivity of copper is $\sigma_{3d} \simeq 5.89 \times 10^7 - j9.14 \times 10^4$ S/m. For an ordinary thin metal tube, $\sigma_{3d}d$ will be on this same order of magnitude if d is on the order of a few nanometers.

We can convert the Pocklington equation (22) into a Hallén's integral equation [2] by writing

$$\left(k^2 + \frac{\partial^2}{\partial z^2}\right)\int_{-L}^{L}(K(z-z')+q(z-z'))I(z')dz' = -j4\pi\omega\varepsilon E_z^i(z) \tag{29}$$

which leads to the function q as

$$q(z-z') = \frac{\omega\varepsilon}{a\sigma}\frac{e^{-jk|z-z'|}}{k}. \tag{30}$$

Assuming a slice-gap source of unit voltage, the final integral equation to solve is

$$\int_{-L}^{L}(K(z-z')+q(z-z'))I(z')dz' = c_1\sin kz + c_2\cos kz$$
$$-\frac{j4\pi\omega\varepsilon}{2k}\sin k|z-z_0| \tag{31}$$

where $c_{1,2}$ are constants to be determined from $I(z \pm L) = 0$. In this paper, a pulse function, point matching solution of (31) is found by expanding the current as

$$I(z) = \sum_{np=1}^{N}I_{np}P_n(z) \tag{32}$$

where $P_{np}(z) = 1$ if $z_{np} - \Delta/2 \leq z \leq z_{np} + \Delta/2$ and $P_{np}(z) = 0$ otherwise, where $z_{np} = -L + (np - (1/2))\Delta$, with Δ being the pulse width, $\Delta = 2L/N$.

Testing at points $z = z_{nt}$, $nt = 1, 2, \ldots, N$, leads to the system of equations

$$\sum_{np=1}^{N}I_{np}Z_{np,nt} = c_1\sin kz_{nt} + c_2\cos kz_{nt}$$
$$-\frac{j4\pi\omega\varepsilon}{2k}\sin k|z_{nt} - z_0| \tag{33}$$

with $nt = 1, 2, \ldots, N$, where

$$Z_{np,nt} = \int_{z_{np}-\frac{\Delta}{2}}^{z_{np}+\frac{\Delta}{2}}\left(\frac{e^{-jk\sqrt{(z_{nt}-z')^2+a^2}}}{\sqrt{(z_{nt}-z')^2+a^2}}\right.$$
$$\left.+\frac{\omega\varepsilon}{a\sigma_{zz}}\frac{e^{-jk|z_{nt}-z'|}}{k}\right)dz'$$
$$= Z_{np,nt}^{(1)} + Z_{np,nt}^{(2)}. \tag{34}$$
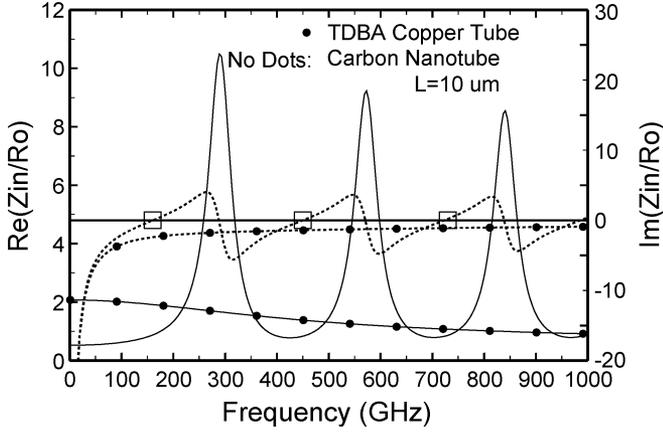
Fig. 4. Input impedance for a carbon nanotube dipole antenna, $m = 40$ ($a = 2.712$ nm), and for a TDBA copper tube dipole having the same radius and length, $L = 10\,\mu$m. Square boxes denote resonance frequencies; solid lines are $\mathrm{Re}(Z_{in}/R_0)$; dashed lines are $\mathrm{Im}(Z_{in}/R_0)$.

Since $I(-L) = I(L) = 0$, $I_1 = I_N = 0$. We can approximate the first integral in (34) as

$$Z_{np,nt}^{(1)} = \begin{cases} \Delta \dfrac{e^{-jkR(z_{np},z_{nt})}}{R(z_{np},z_{nt})}, & nt \neq np \\ 2\ln\left[\dfrac{\Delta}{2a} + \sqrt{1 + \left(\dfrac{\Delta}{2a}\right)^2} - jk\Delta\right], & nt = np \end{cases}$$
(35)

where $R(z_a, z_b) = \sqrt{(z_a - z_b)^2 + a^2}$. In all results, we will assume that the source is located at $z_0 = 0$.

The solution was verified by comparison with the results for imperfectly conducting tubular dipoles [24], [26], [27].

III. RESULTS

The special nature of the carbon nanotube conductivity (9) results in unique properties for carbon nanotube antennas. First, it should be noted that nanoelectronic devices are inherently high-impedance. For example, at the nanoscale, dc electron transport is typically either ballistic [5], exhibiting a quantized resistance on the order of $R_0 = 12.9$ kΩ, or via tunnelling across gaps [28], with an associated high tunneling resistance. Therefore, much as 50 Ω is considered a standard reference impedance for macroscopic antennas, R_0 can be taken as a standard reference impedance for nanoantennas. In the following figures, input impedance values will be normalized to R_0. As will be seen below, carbon nanotubes of reasonable lengths for operation from $F = 1 - 1000$ GHz and beyond will exhibit impedances on this order of magnitude. This is probably a positive attribute, since impedance matching to an impedance on the order of R_0 associated with a nanoelectronic device may be facilitated. In the figures below, dipole antennas having half-length $L = 1\,\mu$m, 10 μm, and 1 mm will be considered, and in all results the dipole radius is $a = 2.712$ nm [corresponding to $m = n = 40$ in (1)]. The main conclusions are that carbon nanotube dipoles exhibit relatively sharp resonances according to the velocity factor $v_p \sim 0.02c$, resonances are suppressed below the relaxation frequency $\nu/2\pi$, and CNs have very low efficiencies compared to macroscale antennas.

In Fig. 4, the normalized input impedance of a CN dipole having half-length $L = 10\,\mu$m is shown. Since a unit voltage slice gap source is assumed, Z_{in} is the reciprocal of the current at the center of the dipole. Also shown are the results for a TDBA copper tube of the same dimensions. As expected, the copper tube dipole does not resonate in this frequency range (a perfectly conducting dipole would resonate at $F = 7500$ GHz; the dipole characterized by σ_{2d} does not resonant at all due to strong damping).

Unlike the copper dipole, the $L = 10\,\mu$m carbon nanotube dipole does resonate in the considered frequency range. These resonances can be associated with plasmons by the transmission line model developed in [12], where the propagation velocity on the antenna was found to be $v_p \simeq 3v_F$ (v_F is taken here to be 9.7×10^5 m/s for CNs [15], although in [12] the value 8×10^5 m/s is quoted). Thus, the transmission-line model predicts that $v_p \simeq 3v_F \simeq 0.01c$, where c is the speed of light in vacuum.[1] Therefore, the wavelength on the antenna should be approximately $\lambda_p \simeq 0.01\lambda_0$, where λ_p is called the plasmon wavelength [12] and λ_0 is the free-space wavelength. As can be seen from Fig. 4, the first resonance of the $L = 10\,\mu$m carbon nanotube antenna is at $F \simeq 160$ GHz. The current distribution at this frequency is approximately a half-wave sinusoid, and thus $2L = \lambda_p/2$, or $\lambda_p = 4L = 40\,\mu$m. Setting $v_p = \lambda_p F$, we obtain $v_p = 0.0213c$, or a velocity reduction factor of $s_r = v_p/c = 0.0213$ at $F = 160$ GHz, which approximately holds at all resonance and antiresonance frequencies shown (in Fig. 4, boxes denote resonance frequencies, based on $\mathrm{Im}(Z_{in}) = 0$ and resonant-like current distributions). Thus, whereas a perfectly conducting metal dipole having half-length $L = 10\,\mu$m would be expected to resonate at $F = 7,500$ GHz, the same length carbon nanotube antenna resonates at $F = 160$ GHz.

The difference between the velocity reduction obtained here $v_p \simeq 0.02c$ and the transmission-line prediction $v_p \simeq 0.01c$ is most likely due to the approximate nature of the transmission-line method, since the L and C values of the two-wire transmission line only approximately hold for the corresponding dipole antenna (thinking of the dipole as a flared-out two-wire line). Furthermore, the transmission-line model does not account for radiation, and only approximately for tube resistance. Thus, the transmission-line model is expected to give valuable yet fairly rough estimates of the actual antenna performance.

A shorter carbon nanotube dipole is considered next, in Fig. 5, where the dipole's half-length is $L = 1\,\mu$m. The first resonance of the carbon nanotube antenna is at $F \simeq 1300$ GHz (yielding $v_p \simeq 0.017c$), and the first antiresonance is at $F \simeq 2,300$ GHz (yielding $v_p \simeq 0.015c$). Additional resonances occur at higher frequencies, but are not shown, although all resonances are due to plasmon effects. Note that a perfectly conducting dipole would resonate at $F = 75\,000$ GHz. As with the $L = 10\,\mu$m antenna, the $L = 1\,\mu$m TDBA copper antenna does not resonate at any frequency due to damping. As can be seen by comparing Figs. 4 and 5, the $L = 1\,\mu$m and $L = 10\,\mu$m carbon nanotube dipoles both resonate in a manner similar to a perfectly conducing dipole, but at resonant

---

[1]There is a typo in [12, (18)]: it should read $v \approx 3v_F \approx 0.01c$, using $v_F = 8 \times 10^5$ m/s.
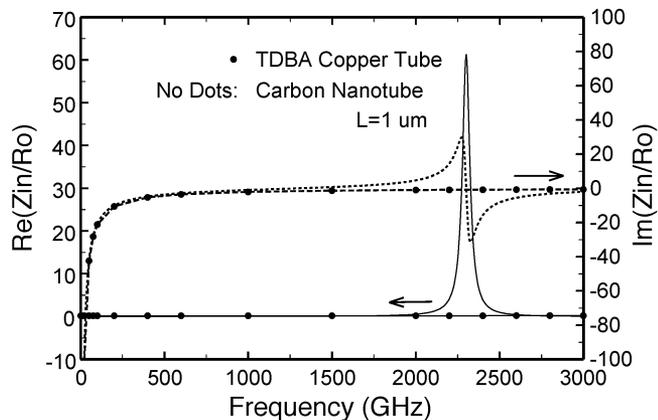
Fig. 5.   Input impedance for a carbon nanotube dipole antenna, $m = 40$ ($a = 2.712$ nm), and a TDBA copper tube dipole having the same radius and length, $L = 1\,\mu$m. Solid lines are $\mathrm{Re}(Z_{in}/R_0)$; dashed lines are $\mathrm{Im}(Z_{in}/R_0)$.
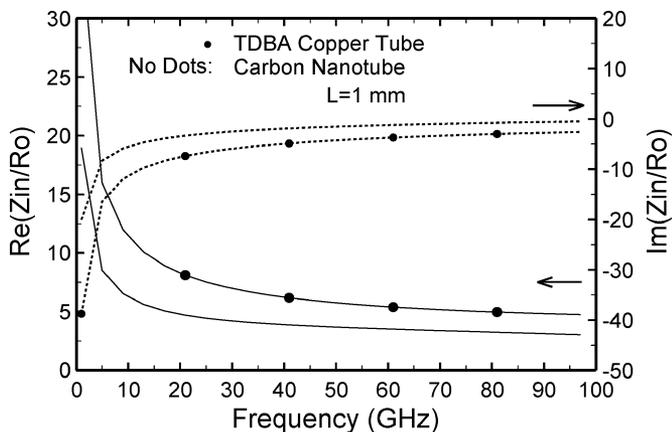
Fig. 6.   Input impedance for a carbon nanotube dipole antenna, $m = 40$ ($a = 2.712$ nm), and for a TDBA copper tube dipole having the same radius and length, $L = 1$ mm. Solid lines are $\mathrm{Re}(Z_{in}/R_0)$; dashed lines are $\mathrm{Im}(Z_{in}/R_0)$.

frequencies corresponding to the velocity reduction factors of $s_r = 0.015$ and $s_r = 0.02$ for the $L = 1\,\mu$m and $L = 10\,\mu$m antennas, respectively.

Plasmon resonances were not observed at the lower frequencies (below the relaxation frequency, roughly 53 GHz). For example, the normalized input impedance of a $L = 1$ mm carbon nanotube antenna, and of a TDBA copper tube antenna, is shown in Fig. 6. A perfectly conducting metal tube dipole having this length would resonant at $F = 75$ GHz, and thus we might expect the carbon nanotube dipole to resonate near $F = 1.6$ GHz, using the velocity reduction factor $s_r = 0.02$ found for the $L = 10\,\mu$m dipole. However, no resonance is evident, consistent with the above discussion. Note that the input impedance values are nevertheless on the order of magnitude of the resistance quantum.

As a further example, Fig. 7 shows Z_{in} versus frequency for several different length CNs. The $L = 10\,\mu$m tube resonates as described previously, and the $L = 20\,\mu$m CN resonates at approximately the value predicted by $v_p = 0.02c$ (i.e., near $F = 75$ GHz, although the first resonance is pushed a bit higher in frequency). However, the $L = 40\,\mu$m CN should resonate at $F = 37$ GHz but does not resonate until a much higher frequency (near $F = 140$ GHz). Thus, it seems clear
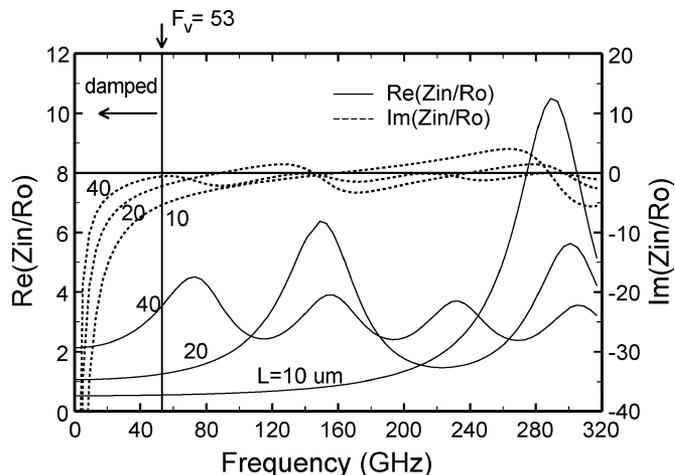
Fig. 7.   Input impedance versus frequency, showing the effect of relaxation frequency damping on antenna resonances.
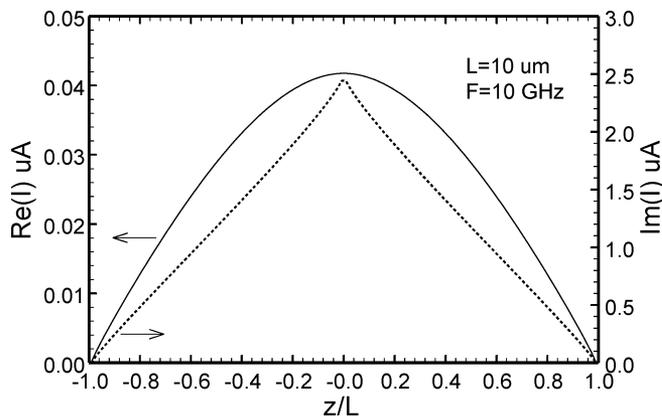
Fig. 8.   Current distribution on a carbon nanotube antenna, $m = 40$ ($a = 2.712$ nm), $L = 10\,\mu$m, $F = 10$ GHz.
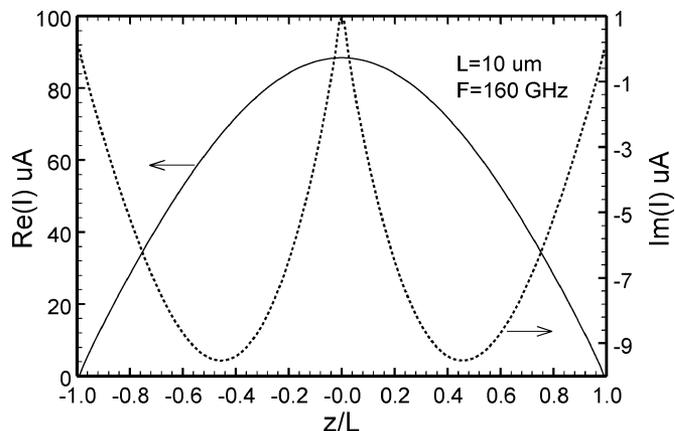
Fig. 9.   Current distribution on a carbon nanotube antenna, $m = 40$ ($a = 2.712$ nm), $L = 10\,\mu$m, $F = 160$ GHz, which is near the first resonance frequency.

that resonances are suppressed below the relaxation frequency $F_\nu = \nu/2\pi$.

Figs. 8–11 show the current distribution on the $L = 10\,\mu$m carbon nanotube dipole at various frequencies. As can be seen from Fig. 8, at frequencies far below resonance, the current distribution is approximately triangular, as for an ordinary short
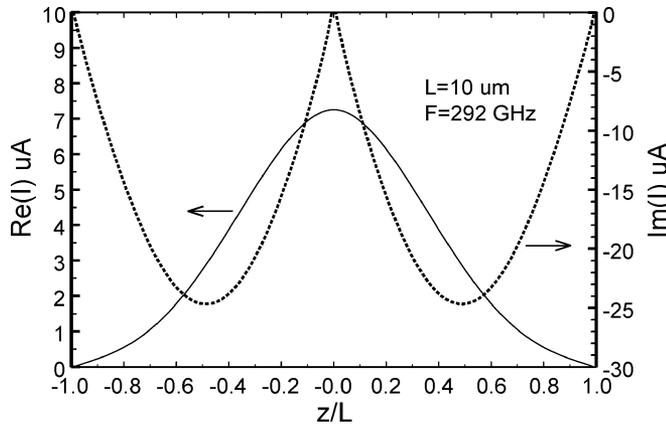
Fig. 10.   Current distribution on a carbon nanotube antenna, $m = 40$ ($a = 2.712$ nm), $L = 10$ μm, $F = 292$ GHz, which is near the first antiresonance frequency.
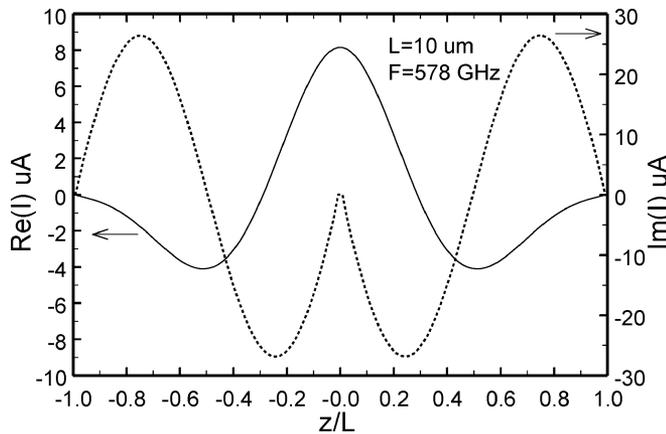
Fig. 11.   Current distribution on a carbon nanotube antenna, $m = 40$ ($a = 2.712$ nm), $L = 10$ μm, $F = 578$ GHz, which is near the second antiresonance frequency.

Fig. 12.   Current distribution on a carbon nanotube antenna, $m = 40$ ($a = 2.712$ nm), $L = 1$ mm, $F = 10$ GHz.

Fig. 13.   Normalized magnitude of the current on an $L = 10$ μm dipole at different relaxation times, showing the influence of damping.

TABLE II
INPUT IMPEDANCE AND EFFICIENCY FOR A CARBON NANOTUBE HAVING $L = 10\mu$m AND $a = 2.712$ nm AT VARIOUS FREQUENCIES

Frequency (GHz)	Z_{in}/R_0	$e_r = P_r/P_{in}$
10	$0.527 - j31.24$	1.2×10^{-8}
160	$0.876 - j0.014$	3.3×10^{-6}
292	$10.46 - j1.48$	1.1×10^{-5}
450	$0.83 + j0.0058$	2.6×10^{-6}

dipole. Fig. 9 shows the current near the first resonance, where it is seen that the current is approximately a half-sinusoid. Figs. 10 and 11 show the current near the first two antiresonances. Current profiles on the same size TDBA copper antenna are quite different, but are not shown (on these antennas, as frequency is raised starting at 10 GHz, the current magnitude transitions from being approximately triangular to becoming strongly damped, without exhibiting any resonance effects).

For the $L = 1$ mm CN dipole antenna, the current distribution at $F = 10$ GHz is shown in Fig. 12. In accordance with the preceding discussion, it can be seen that the current is strongly damped at this frequency and does not show resonance effects.

Finally, the effect of relaxation frequency on the current distribution is shown in Fig. 13 for the $L = 10$ μm dipole at $F = 160$ GHz (i.e., near its first resonance when $\tau = 3$ ps). Although τ in the range of 3–0.3 ps is typical of carbon nanotubes, smaller τ are also shown for illustrative purposes.

It can be seen that relaxation phenomena are very important at the frequencies of interest here (gigahertz to terahertz range). Although above approximately $F_\nu = 53$ GHz (when $\tau = 3$ ps) the carbon nanotube dipole shows relatively sharp resonance behavior, ohmic losses can nevertheless be quite high due to

the extremely small radius of the tube. This is somewhat unavoidable for dipoles having nanometer radius values, and this aspect will generally impact antennas for communicating with nanocircuits. This topic will be considered in more detail elsewhere, although some results for the efficiency of a carbon nanotube having $a = 2.712$ nm at various frequencies are given in Table II. The efficiency is on the order of 10^{-5} to 10^{-6} at most frequencies. Although not included in the table, for the $L = 1$ μm dipole, the efficiency was slightly better, although still on the order of 10^{-5}. For shorter dipoles, $e_r \sim 10^{-4}$ was found at terahertz frequencies, although this matter warrants further study. However, despite these extremely low values of efficiency, many of the currently envisioned nanoelectronic devices

are sensitive to the movement of a single electron, or of a few electrons (the so-called "single electron" devices), and these low efficiencies may nevertheless be adequate for electromagnetic interaction with nanocircuits.

Although not shown, the radiation pattern for all carbon nanotube antennas considered here is essentially that of a very short dipole (i.e., $E_\theta, H_\phi \sim \sin\theta$). This is true even when the current has many oscillations (which, in the case of a perfectly conducting dipole, would lead to a more complicated, usually multilobed far-field pattern). This can be understood physically since, despite the influence of the velocity reduction along the antenna, the antenna is still very short compared to the free-space wavelength. Radiation into space essentially occurs from an electrically small region around the origin, and, hence, the pattern is that of a small dipole. Mathematically, this can easily be shown since the field is calculated from an integration of the current over the dipole length $2L$, and involves the free-space wavenumber k. Since kL is very small (for the numerical solution, corresponding factors involving $k\Delta$ and kz_{np} arise), the $\sin\theta$ pattern emerges. Thus, the directivity of the carbon nanotube antennas considered here is approximately $D = 1.5$, although the gain G will be small due to the small value of efficiency ($G = e_r D$).

It should be noted that, at this point, it is not clear what types of devices, or transmission lines, may be used to connect to a carbon nanotube antenna, although a natural choice would be a carbon nanotube transmission line feeding some sort of nanoelectronic circuit. For example, in [29], small antennas (having lengths on the order of 50 μm) are proposed for receiving terahertz radiation. Received power would be rectified to provide dc power to microscopic or nanoscopic circuits (including untethered microscopic/nanoscopic robots). In [12], nanoantennas are suggested to solve the nanointerconnect problem—that is, how to connect the "outside world" to a nanoscopic system. It seems clear that antennas on the order of micrometers, give or take a few orders of magnitude, will play an increasing important role in research and future applications. As such, this paper represents a very preliminary investigation into the fundamental radiation properties of dipole antennas constructed from carbon nanotubes.

IV. CONCLUSION

Fundamental properties of dipole transmitting antennas formed by carbon nanotubes have been investigated via a Hallén's-type integral equation. The equation is based on a semiclassical conductivity, equivalent to a more rigorous quantum mechanical conductivity at the frequencies of interest here. Properties such as the input impedance, current distribution, and radiation pattern have been discussed, and comparisons have been made to a copper antenna having the same dimensions. It is found that, due to properties of the carbon nanotube conductivity function, and its relationship to plasmon effects, some properties of carbon nanotube antennas are quite different from the case of an infinitely thin copper antenna of the same size and shape. Important conclusions of this paper are that carbon nanotube antennas are found to exhibit plasmon resonances above a sufficient frequency, have high

input impedances (which is probably beneficial for connecting to nanoelectronic circuits), and exhibit very low efficiencies.

REFERENCES

[1] I. Iijima, "Helical microtubules of graphitic carbon," *Nature*, vol. 354, pp. 56–58, 1991.

[2] S. Li, Z. Yu, C. Rutherglan, and P. J. Burke, "Electrical properties of 0.4 cm long single-walled carbon nanotubes," *Nano Lett.*, vol. 4, pp. 2003–2007, 2004.

[3] R. Saito, G. Dresselhaus, and M. S. Dresselhaus, *Physical Properties of Carbon Nanotubes*. London, U.K.: Imperial College Press, 2003.

[4] Z. Yao, C. Dekker, and P. Avouris, "Electrical transport through single-wall carbon nanotubes," in *Carbon Nanotubes; Topics in Applied Physics*, M. S. Dresselhaus, G. Dresselhaus, and P. Avouris, Eds. Berlin, Germany: Springer-Verlag, 2001, vol. 80, pp. 147–171.

[5] S. Datta, *Electronic Transport in Mesoscopic Systems*. Cambridge, U.K.: Cambridge Univ. Press, 1995.

[6] S. Li, Z. Yu, S. F. Yen, W. C. Tang, and P. J. Burke, "Carbon nanotube transistor operation at 2.6 GHz," *Nano Lett.*, vol. 4, pp. 753–756, 2004.

[7] J. P. Clifford, D. L. John, L. C. Castro, and D. L. Pulfrey, "Electrostatics of partially gated carbon nanotube FETs," *IEEE Trans. Nanotechnol.*, vol. 3, pp. 281–286, Jun. 2004.

[8] K. G. Ong, K. Zeng, and C. A. Grimes, "A wireless, passive, carbon nanotube-based gas sensor," *IEEE Sensors J.*, vol. 2, pp. 82–88, 2002.

[9] P. Kim and C. M. Lieber, "Nanotube nanotweezers," *Science*, vol. 286, pp. 2148–2150, 1999.

[10] G. Pirio, P. Legagneux, D. Pribat, K. B. K. Teo, M. Chhowalla, G. A. J. Amaratunga, and W. I. Milne, "Fabrication and electrical characteristics of carbon nanotube field emission microcathodes with an integrated gate electrode," *Nanotechnology*, vol. 13, pp. 1–4.

[11] P. J. Burke, "Lüttinger liquid theory as a model of the GHz electrical properties of carbon nanotubes," *IEEE Trans. Nanotechnol.*, vol. 1, pp. 129–144, Sep. 2002.

[12] P. J. Burke, S. Li, and Z. Yu, "Quantitative theory of nanowire and nanotube antenna performance," *IEEE Trans. Nanotechnol.*, submitted for publication.

[13] P. J. Burke, "An RF circuit model for carbon nanotubes," *IEEE Trans. Nanotechnol.*, vol. 2, pp. 55–58, Mar. 2003.

[14] J. J. Wesström, "Signal propagation in electron waveguides: Transmission-line analogies," *Phys. Rev. B*, pp. 11 484–11 491, Oct. 1996.

[15] S. A. Maksimenko, G. Y. Slepyan, A. Lakhtakia, O. Yevtushenko, and A. V. Gusakov, "Electrodynamics of carbon nanotubes: Dynamic conductivity, impedance boundary conditions, and surface wave propagation," *Phys. Rev. B*, vol. 60, pp. 17 136–17 149, Dec. 1999.

[16] S. A. Maksimenko and G. Y. Slepyan, "Electrodynamic properties of carbon nanotubes," in *Electromagnetic Fields in Unconventional Materials and Structures*, O. N. Singh and A. Lakhtakia, Eds. New York: Wiley, 2000.

[17] G. W. Hanson, "Fundamental transmitting properties of carbon nanotube antennas," in *IEEE Int. Symp. Antennas Propagation*, Washington, DC, Jul. 2–3, 2005.

[18] M. S. Roglski and S. B. Palmer, *Solid State Physics*, Australia: Gordon and Breach, 2000.

[19] C. Kittel, *Introduction to Solid State Physics*, 6th ed. New York: Wiley, 1986.

[20] A. P. Sutton, *Electronic Structure of Materials*. Oxford, U.K.: Clarendon, 1993.

[21] G. W. Hanson, *Introduction to Nanoelectronics*. Englewood Cliffs, NJ: Prentice-Hall, to be published.

[22] R. S. Elliott, *Antenna Theory and Design*. Englewood Cliffs, NJ: Prentice-Hall, 1981.

[23] G. Fikioris, "On the application of numerical methods to Hallén's equation," *IEEE Trans. Antennas. Propag.*, vol. 49, pp. 383–392, Mar. 2001.

[24] R. W. P. King and T. T. Wu, "The imperfectly conducting cylindrical transmitting antenna," *IEEE Trans. Antennas. Propag.*, vol. AP-14, pp. 524–534, Sep. 1966.

[25] W. Steinhögl, G. Schindler, G. Steinlesberger, M. Traving, and M. Engelhardt, "Comprehensive study of the resistivity of copper wires with lateral dimensions of 100 nm and smaller," *J. Appl. Phys.*, vol. 97, pp. 023 706(1)–023 706(7), 2005.

[26] C. D. Taylor, C. W. Harrison, and E. A. Aronson, "Resistive receiving and scattering antenna," *IEEE Trans. Antennas. Propag.*, vol. AP-15, pp. 371–376, May 1967.

[27] B. D. Popović and Z. D. Popović, "Imperfectly conducting cylindrical antenna: variational approach," *IEEE Trans. Antennas. Propag.*, vol. AP-19, pp. 435–536, May 1971.

[28] D. K. Ferry and S. M. Goodnick, *Transport in Nanostructures*. Cambridge, U.K.: Cambridge Univ. Press, 1999.

[29] P. H. Siegel, "Nanoconverters for powering nanodevices," *NASA Tech. Brief*, vol. 27, no. 3, 2003.

G. W. Hanson (S'85–M'91–SM'98) was born in Glen Ridge, NJ, in 1963. He received the B.S.E.E. degree from Lehigh University, Bethlehem, PA, the M.S.E.E. degree from Southern Methodist University, Dallas, TX, and the Ph.D. degree from Michigan State University, East Lansing, in 1986, 1988, and 1991, respectively.

From 1986 to 1988, he was a Development Engineer with General Dynamics, Fort Worth, TX, where he worked on radar simulators. From 1988 to 1991, he was a Research and Teaching Assistant in the Department of Electrical Engineering, Michigan State University. He is currently an Associate Professor of electrical engineering and computer science at the University of Wisconsin, Milwaukee. His research interests include electromagnetic wave phenomena in layered media, integrated transmission lines, waveguides and antennas, leaky waves, and mathematical methods in electromagnetics.

Dr. Hanson is a Member of the International Scientific Radio Union (URSI) Commission B, Sigma Xi, and Eta Kappa Nu. He is an Associate Editor for the IEEE TRANSACTIONS ON ANTENNAS AND PROPAGATION.